

## Design model for dry-stacked and demountable masonry blocks

Gelen Gael Chewe Ngapeya<sup>1</sup>, Danièle Waldmann<sup>1</sup>

1 University of Luxembourg, 6 Avenue de la Fonte, L-4364 Esch/Alzette, (+352) 46 66 44 5279, danielle.waldmann@uni.lu

[Abstract]. The construction industry around the world produces a large part of inert wastes mainly coming from building demolitions. Facing to this environmental challenge and considering the new policy initiatives supporting the designing of sustainable buildings, dry-stacked masonry comes forward as a promising solution since components can be dismantled, saved in a component bank and reassembled on new sites. The speedy growth of the construction industry, the increasing importance given to the complete life cycle of buildings and the evolution of construction technics have led to the development of dry-stacked masonry structures. Mortarless masonry structures minimise skilled labour requirements and improve construction productivity. However, despite these advantages, there are no design standards providing guidelines to assess the load-bearing capacity of dry-stacked masonry block, which therefore limits its use in construction. In an attempt to fill this lack, the current paper investigates the load-bearing capacity of dry-stacked masonry and its influencing parameters. The effects of the geometric imperfections such as height imperfections and bed-joint roughness have been analysed as well as a mitigation strategy. Then, based on experimental evidence, a design method has been proposed for dry-stacked masonry solicited by axial compression. The developed design methodology provided promising results, with 93% of accuracy in the prediction of the dry-stacked masonry's load-bearing capacity.

**Keywords:** dry-stacked masonry, Load-bearing capacity, Geometric imperfections



## 1 Introduction

In the last decades, large-scale demolition and reconstruction of old urban areas have been observed, producing a significant part of inert waste materials around the world. During deconstruction or at the end of life, traditional mortared masonry walls offer no other recycling paths than demolition. Conversely, demountable construction systems like dry-stacked masonry bring forward twofold main assets: (i) the ease and speed of execution, which directly affects the construction cost; and (ii) the demountability, which positively affects the ecological impact by offering a second life to masonry blocks. (Bari, Abdullah, Yusuff, Ismail, & Jaapar, 2012) and (Anand & Ramamurthy, 2003) investigated the effectiveness of the dry-stacked masonry system in the construction productivity. They evidenced that the use of a dry-stacked masonry system leads to an enhancement of the productivity by 80 to 100% compared to a traditional mortared masonry system. The measurement made by (Anand & Ramamurthy, 2003) regarding the net output of 1 m<sup>2</sup> of wall per productive hour while using different masonry systems is reported as a radar in Fig. 1. They evidenced that dry-stacked systems are more effective than a traditional system in terms of productivity.

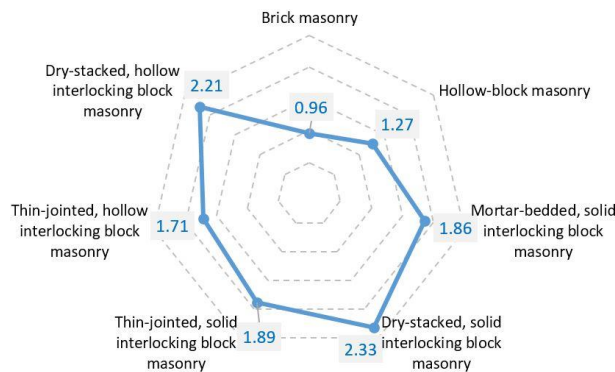


**Fig. 1 Construction net output of 1 m<sup>2</sup> of wall per productive hour for different masonry systems (figure made using the data of (Anand & Ramamurthy, 2003))**

In view of this productivity performance, researchers have made intensive efforts for developing dry-stacked masonry systems to make masonry construction more affordable and sustainable. Thus, several dry-stacked masonry blocks have been designed worldwide with different interlocking mechanisms (Abang Ali, 1987; Agaajani, Waldmann, Scholzen, & Louge, 2016; Ben Ayed, Limam, Aidi, & Jelidi, 2016; Cetholic, 1988; Haener, 1984; Sturm, Ramos, & Lourenço, 2015; Thallon R, 1983; W. A. Thanoon et al., 2004). The interlocking mechanism improves the vertical and horizontal alignment of walls and provides a certain out-of-plan resistance to walls in the absence of the mortar layer.

Nonetheless, although the dry-stacked masonry system offers attractive interests, its extensive use is still hindered by (i) the premature cracking of wall which is related to the effect of the block geometric imperfections; and (ii) the lack of appropriate design standards for safely predicting its load-bearing capacity. In the current state-of-art, a couple of investigations first characterised the geometric imperfections of dry-stacked blocks as being the height difference and bed-joint roughness (Agaajani et al., 2016; Allaoui, Rekik, Gasser, Blond, & Andreev, 2018; Andreev et al., 2012; Gelen Gaël Chewé Ngapeya & Waldmann, 2020; Gasser, Terny-Rebeyrotte, & Boisse, 2004; Mohd Saleh Jaafar; Ahmed Alwathaf; Waleed Thanoon; J. Noorzaei; M. R. Abdulkadir, 2006). Then, the authors measured the imperfections using different technics like the matrix-based tactile surface sensors, the Fujifilm strips, the carbon footprint paper, the digital image correlation and the standard displacement sensors. From the different measurements, it emerged that the height difference between dry-stacked masonry blocks varies between +/- 0,25 and 2 mm, while the height of the asperities in the bed-joint roughness falls between 0,03 and 0,25 mm.

The lack of mortar layers in the horizontal joints of interlocking masonry walls combined to geometric imperfections of blocks lead to structural behaviour fundamentally different from conventional masonry walls under axial compression. (Bigoni & Noselli, 2010a) carried out investigations on dry-stacked masonry under axial compression. Upon the loading, they captured the actual load percolation system using the photo-elasticity transmission technic. They evidenced a tree-like load percolation system occurring in a dry-stacked masonry wall. They also revealed that the load

transfer from course to course occurs in the middle and the edge sections of blocks, which results in high-stress peaks in dry-stacked masonry walls. The authors also observed that the highly localised stress percolation system observed in the first stages of the loading gradually tends towards a wider stress distribution in the last loading stages, a result of the increase of the contact surfaces in the wall as demonstrated by (Gelen Gael Chewe Ngapeya & Waldmann, 2020; Zahra & Dhanasekar, 2018). In further investigations, the authors (Bigoni & Noselli, 2010b) proposed a simple analytical model for determining the intensity of loads transmitted on blocks as a function of a predefined load transmission mechanism in the dry-stacked masonry wall.

(W. A. M. Thanoon, Alwathaf, Noorzaei, Jaafar, & Abdulkadir, 2008) performed numerical and experimental investigations on a 3-course dry-stacked masonry prism for discussing the mechanical behaviour under axial compression. First, they constructed a dry-stacked masonry prism in the lab and measured its stress-deformation response under axial compression. They observed (i) a nonlinear stress-deformation curve with a flat part related to the closure of gaps in the bed-joints, (ii) a progressive inflection of the measured curve related both to the crushing of the asperities and the increase of the actual contact, and (iii) a flat and oblique curve part related to the achievement of the maximum contact stiffness in the bed-joints. Then, they computed the corresponding contact stiffness of the bed-joints, which they imported in their finite element model for indirectly consider the effect of the bed-joint roughness on the overall mechanical behaviour of the masonry prism. After running their numerical model, they found that under compression dry-stacked masonry suffers from asymmetric stress distribution in the face-shells of blocks. In addition, they demonstrated that dry-stacked masonry suffers from surface roughness related stress concentration, which strongly reduces its load-bearing capacity. Their results confirms the findings of (Ben Ayed et al., 2016; Kang-Ho Oh; Harry G. Harries; Ahmed A. Hamid, 1995; Lourenço, Oliveira, Roca, & Orduña, 2005; Lourenço & Ramos, 2004). In an attempt to guide the prediction of the load-bearing capacity of dry-stacked masonry walls, several other authors developed correlations between block strength and masonry wallet/prism strength (Jaafar, Thanoon, Najm, Abdulkadir, & Ali, 2006; Silva et al., 2015; Sturm et al., 2015). A review of the proposed correlations revealed that the prism/wallet to block strength ratio varies between 0,21 and 0,70. Although being of significant value, the strength correlations cannot be directly used for designing dry-stacked masonry walls since the influence of the block imperfections strongly varies with the size of both blocks and walls.

The present investigation has a twofold perspective of (1) settling a design model for dry-stacked masonry and (2) assessing a mitigation strategy to overcome the impact of the geometric imperfections of block units on the load-bearing capacity of walls.

## **2 Methodology**

In the framework of this investigation, the methodology adopted to set up a design model for dry-stacked masonry was organised in three stages. In the first stage, experimental tests were carried out on wallets with a dual purpose: (i) to assess the effectiveness of the mitigation strategy for improving the load-bearing capacity of dry-stacked masonry and (ii) to constitute an experimental database useful for developing a reliable design model. In the second stage, the results of the experimental tests were combined with a statistical modelling of the impact of the geometrical imperfections of block units to settle down a design model for dry-stacked and demountable masonry. In the third and last stage, a design model was implemented to compute the load-bearing capacity of dry-stacked masonry walls and to compare the findings to the test results found in literature.

### **2.1 Raw dry-stacked masonry**

The investigations on the load-bearing capacity of dry-stacked masonry and the influence of the geometric imperfections of the block units have been carried out on a block delivered by a local producer. The used masonry block was made of two load-bearing face-shells with a net cross-section of 22.000 mm<sup>2</sup>, interconnected by two webs (Fig. 2). The masonry block has a nominal height, length and thickness of 200 mm, 500 mm and 200 mm respectively, with a self-weight of 20 kg. In the first stage of the experimental analysis, following the provisions of the British Standards EN 772-1 (*BS EN 772-1:2000, Methods of test for masonry units – Part 1: Determination of compressive strength*, n.d.), uniaxial compressive tests have been realised on 10 randomly selected masonry blocks for the purpose of mechanical characterisation. The masonry blocks exhibited a mean compressive strength of 13 MPa.



**Fig. 2 Masonry block** (Gelen Gaël Chewe Ngapeya & Waldmann, 2020)

## 2.2 Improved dry-stacked masonry

In the framework of the development of a design model for dry-stacked and demountable masonry, a mitigation strategy was also analysed for overcoming the curtailing effect of the geometric imperfections of blocks on the overall load-bearing capacity of walls. Indeed, (Zahra & Dhanasekar, 2018) have evidenced that the strong stress peaks generally observed in dry-stacked masonry systems can be partially relieved effortlessly by embedding a compressible material in the contact interfaces. As a mitigation strategy, a 10 mm layer of soft material was applied on the top faces of the block face-shells, with the aim to dampen or level the geometric imperfections of raw dry-stacked masonry blocks. The definition of the thickness of the additional layer was mainly based on the works of (Tang, 2012) who studied the effect of mortar thickness on the compressive strength of brick masonry. In fact, the author demonstrated that the optimum mortar thickness leading to the least effect on the masonry's strength is 10 mm.

For applying the additional material layer, the hardened masonry blocks were re-moulded in formworks heightened by 10 mm around the block face-shells. The empty space forecasted on the face-shells was then filled by hand with fresh mixed and purposely selected materials, before being slightly vibrated. The improved dry-stacked masonry blocks were then stored 28 days for hardening purpose.

## 3 Experimental analysis of the contact network and the load-bearing capacity of masonry walls

### 3.1 Materials of the additional layer

(Vasconcelos & Lourenço, 2009) carried out experimental characterisations of stone masonry in shear and compression and revealed that the bed-joint closure in dry-stacked masonry is proportional to the contacting material stiffness. The closure of the bed-joint being strongly relates to the rate of the actual contact in the contact interfaces while the ultimate resistance of dry-stacked masonry still closely relates to the rate of the actual contact in the contact interfaces (Gelen Gael Chewe Ngapeya, Waldmann, & Scholzen, 2018). The selection of the material for the additional layer was of high significance. Indeed, four materials of different mechanical properties have been chosen. Three materials of a relatively common strength but of decreasing Young's modulus (Mix A, Mix B and Mix C) were compared to a very low strength material (Mix D). Low strength materials are known to induce significant lateral tensile stresses in dry-stacked masonry, which might limit the overall ultimate load-bearing capacity of walls. Despite that, it has been chosen for its possible high expectation of levelling capacity of block imperfections. On the other hand, although they might lead to less levelling of block imperfections, medium strength materials have been chosen as they are known to induce less lateral tensile stresses and higher load-bearing capacity in mortared masonry (Mohamad, Fonseca, Vermeltfoort, Martens, & Lourenço, 2017; Zucchini & Lourenço, 2007).

The compressive strength of the four mixes used for the additional layer was determined on prism samples of 4 x 4 x 16 cm following the recommendations of the British standard EN 1015-11, the stress-strain behaviour has been captured as well. The results of the experimental tests are summarised in Table 1.

**Table 1: Compressive strength and Young's Modulus of different variations of the additional layer**

Mixture	Mean compressive strength (N/mm <sup>2</sup> )	Young's Modulus (MPa)
Mix A	37,0	11500
Mix B	34,0	10500
Mix C	38,0	7000
Mix D	5,2	3000

### 3.2 Test design on masonry wall and prism.

The experimental program sought to investigate the impact of the different materials of the additional layer on the levelling of the bed-joint imperfections and ultimately on the load-bearing capacity of dry-stacked masonry walls. The following questions were raised:

- Which mixes of the additional layer achieve a high actual contact in the bed-joint?
- To what extend the load-bearing capacity of a dry-stacked masonry wall with improved blocks can be increased with respect to a similar one with raw dry-stacked masonry blocks?

For the purpose to answer to these questions, two test series have been designed. In the first series, 25 masonry prisms constituted each of a dry-stacking of three blocks were investigated to singularly analyse the impact of the bed-joint roughness on the actual contact. The actual contact in the bed-joints was captured using Fujifilm strips. Indeed, Fujifilm strips are a type of sensors able to record the footprint and the intensity of the contact at the interface between solids. The Fujifilm strips were inserted at the interface between the masonry blocks during the prism erection. Afterwards, the prism specimens were axially compressed to failure using a couple of six hydraulic pistons as showed in Fig. 3. Thereafter, the Fujifilm strips were retrieved, digitalised and processed on MATLAB for computing the maximum rate of the actual contact recorded in the bed-joints. In the second series, 20 masonry wallets of 0,8 m height and 1,0 m length were tested (Fig. 3). Indeed, masonry wallets were investigated because they better depict the behaviour of dry-stacked masonry, since they include effects of both bed-joint roughness and height difference of blocks. Like for the masonry prisms, the wallets were also axially compressed to failure. The ultimate load was monitored. In addition, cameras were used to record and further analyse the failure mechanism of the wallets.

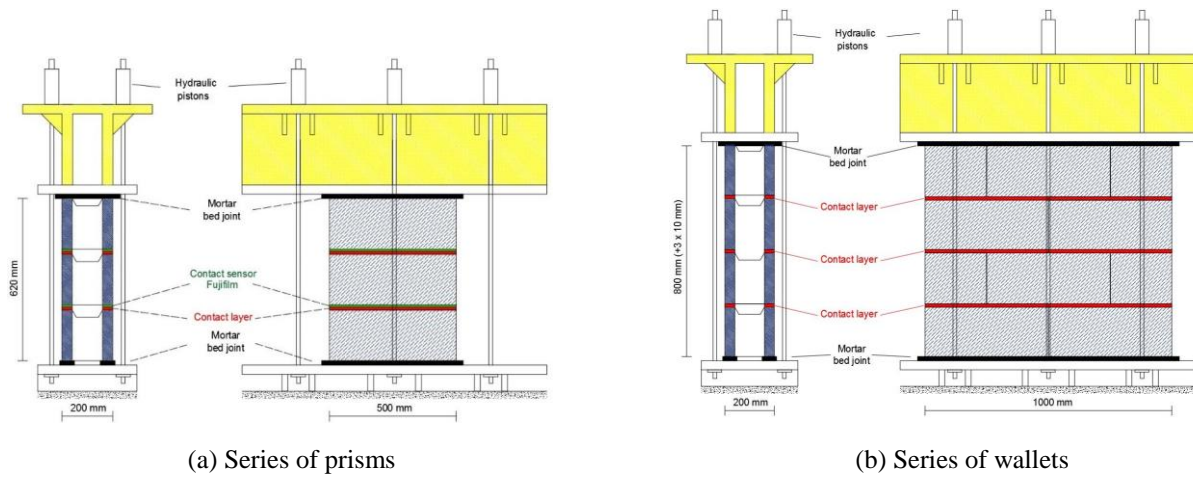


**Fig. 3 Design of the experimental tests on (a) prisms and (b) masonry wallets** (Gelen Gaël Chewé Ngapeya & Waldmann, 2020)

### 3.3 Results.

The mean rates of the actual contact measured in the bed-joints of the masonry prisms are summarized in Table 2. A huge reduction of the nominal contact section has been observed in the masonry prisms with raw blocks (group I), with only 23% of actual contact. This could have been foreseen since the parts of the masonry blocks coming into contact exhibit a same and high stiffness, which results in a very low deformation of the asperities at the interface and ultimately a very low contact. Regarding the masonry prisms with blocks improved with Mix A and Mix B (group II and group III respectively), a significant improvement was observed about the actual contact. Indeed, the actual contact has been doubled and achieved up to 50%, thanks to a higher deformation and crushing of the asperities at the interfaces. A similar tendency was observed for the masonry prisms with blocks improved with Mix C (group IV). In this case, the low Young's Modulus of Mix C even still allowed to slightly increase the actual contact to 55%. In the last case where the blocks of the masonry prisms were improved with Mix D (Group V), although this material of the contact layer had the lowest Young's Modulus, the resulting actual contact was just about 40%. This performance was better than the one of group I but still less than the ones of group II, III and IV. The default of higher performance of the masonry prisms of group II, III and IV was due to the reduction of the load-bearing capacity related the significant lateral tensile stresses induced in the masonry prisms.

As a summary of the tendency observed from prisms with raw blocks to prisms with improved blocks, it can be stated that the lower the stiffness of the parts coming into contact, the higher the resulting actual contact in the interface, which lines up with the finding of (Vasconcelos & Lourenço, 2009).

**Table 2: Mean rate of the actual contact in the bed-joints of masonry prisms**

Mixture	Number of prisms tested	Mean rate of the actual contact	Coef. of variation
Group I – prisms with raw blocks (no additional layer)	5	23%	4%
Group II – prisms with blocks improved using Mix A	5	50%	7%
Group III – prisms with blocks improved using Mix B	5	50%	8%
Group IV – prisms with blocks improved using Mix C	5	55%	8%
Group V – prisms with blocks improved using Mix D	5	40%	7%

The load-bearing capacity of the tested wallets is summarised in Table 3. The wallets of group I made with raw dry-stacked masonry blocks showed a load bearing capacity of about  $3,66 \text{ N/mm}^2$ . In the wallets of group II and III, it was only improved by 1,0% and 6,1% respectively, which is not relevant for engineering purposes. The impact of the additional layer was balanced between the positive aspect related to the increase of the actual contact, hence the better stress distribution, and the negative aspect related to the induction of lateral tensile stress in lateral masonry block walls, leading to a premature cracking of the webs. A considerable structural improvement could be observed for the wallets of group IV, with an increase of the load-bearing capacity of 31,9%. This largely results from the high levelling capacity of the additional layer material. Both block height difference and bed-joint roughness were significantly overcome. In the last group, the load-bearing capacity was diminished 41,3%, due to the significant lateral tensile stress induced by the low strength material Mix D in the wallets.

**Table 3: Load-bearing capacity of the wallets**

Mixture	Number of wallets tested	Mean load-bearing capacity $P_u (\text{N/mm}^2)$	Improvement
Group I – prisms with raw blocks (no additional layer)	4	3,66	-
Group II – prisms with blocks improved using Mix A	4	3,70	+1,0%
Group III – prisms with blocks improved using Mix B	4	3,88	+6,1%
Group IV – prisms with blocks improved using Mix C	4	4,83	+31,9%

Throughout the experimental campaign, three damage mechanisms have been observed prior to the wall collapse. Consecutively, it was first the face-shells splitting due to the height difference between the blocks and occurring around 17% to 92% of the load-bearing capacity. Then, it was the spalling of some sections of the face-shells near the bed-joints, due to the high-stress concentration resulting from the tree-like load percolation system (Gelen Gael Chewe Ngapeya et al., 2018). This damage mechanism occurred generally after 70% of the load-bearing capacity. The third and last damage mechanism occurring near the failure was the cracking at the interface between the face-shells and the webs of blocks. This latter one was mainly due to the development of significant lateral tensile stress in the masonry blocks.

#### 4 Design model

To date, the standards for the design of masonry structures only provide guidelines for traditional and thin-mortared masonry. As shown in equation (1) recommended by EN 1996-1-1(EC6), the compressive strength of mortared masonry is calculated while considering exclusively the safety factor  $\gamma_M$ , the slenderness effect  $\phi$ , the masonry block thickness  $t$ , the normalised compressive strength of blocks  $f_b$ , the mortar compressive strength  $f_m$  and a coefficient K, which depends on the block material (concrete, clay, brick, etc). In equation (1), for thin mortared masonry  $\alpha = 0,85$  and  $\beta = 0$ , while for traditional mortared masonry  $\alpha = 0,7$  and  $\beta = 0,3$ .

$$N_{Rd. \text{EN}1996-1-1} = \frac{1}{\gamma_M} (\phi t K f_b^\alpha f_m^\beta) \quad (1)$$

For developing a design model for dry-stacked masonry, the proposal of equation (1) was exploited and extended by including two new factors involving the impact of the geometric imperfections of blocks on the overall compressive strength of walls. Equation (2) stands for dry-stacked masonry walls with raw blocks, whereas equation (3) stands for walls with improved blocks. Moreover, in these proposals,  $\delta_h$  and  $\delta_r$  stand for the reduction factor due to the height variation and the reduction factor due to the bed-joint roughness respectively. Given that in a wall the effects of the two geometric imperfections are coupled, each design model was defined to fit the best with the experimental results and this was then validated with the results of former experiments collected in literature.

$$N_{Rd. \text{proposed}} = \frac{1}{\gamma_M} (\phi t K f_b^{0,95}) \delta_h^{0,85(1-\delta_r)} \quad (2)$$

$$N_{Rd. \text{proposed}} = \frac{1}{\gamma_M} (\phi t K f_b^{0,85} f_m^{0,2}) \delta_h^{0,85(1-\delta_r)} \quad (3)$$

##### 4.1 Factor $\delta_r$

Standing for the impact of the bed-joint roughness, the factor  $\delta_r$  is defined as being the ratio between the maximum surface of actual contact achieved in a bed-joint and the nominal contact surface. Hence, the impact of the bed-joint roughness was indirectly measured during the experimental tests on the masonry prisms. The mean rate of the actual contact defined in Table 2 is here considered as being the factor  $\delta_r$  for each type of masonry blocks.

##### 4.2 Factor $\delta_h$

The determination of factor  $\delta_h$  standing for the impact of the height difference between masonry blocks is mainly based on a developed deterministic model. Indeed,  $\delta_h$  depicts the overall reduction of the useful section of a wall due to a reduction of the contact surface due to imperfections. As demonstrated in several investigations (Agaajani et al., 2016; Bigoni & Noselli, 2010a; Gelen Gael Chewe Ngapeya et al., 2018), the height difference between dry-stacked masonry blocks strongly impacts the contact network and systematically leads to a major tree-like ramification through which the load percolates. Concisely, for a given wall, factor  $\delta_h$  was defined as being the ratio between the total actual contact through which the load percolates and the total nominal contact sections of the wall. However, since the load percolation system might vary from one wall to another according to a random distribution of blocks, the factor  $\delta_h$

might also vary from one wall to another of same geometry. To consider this,  $n$ -walls different walls have been analysed within a deterministic model. With a number  $n = 1000$  a quasi-steady value of  $\delta_h$  for a given wall geometry has been found.

For engineering purposes, a designer's diagram was developed using a MATLAB code for determining the factor  $\delta_h$ . More details are provided in (Gelen Gaël Chewe Ngapeya & Waldmann, 2020). The designer's diagram is here presented in Fig. 4.

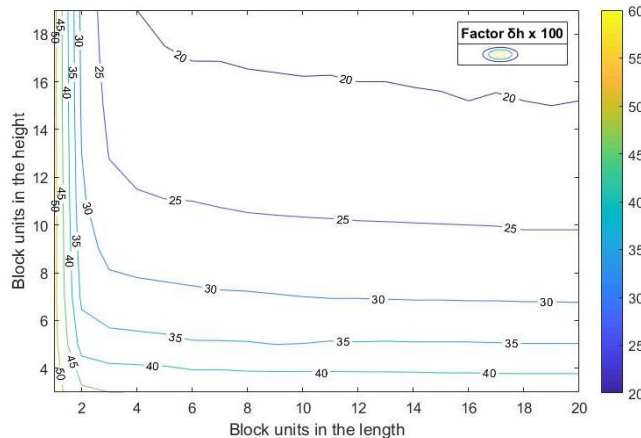


**Fig. 4** Designer's diagram for the determination of  $\delta_h$  (Gelen Gaël Chewe Ngapeya & Waldmann, 2020)

#### 4.3 Implementation

In the present sub-section, the load-bearing capacity of dry-stacked masonry walls are computed using the proposed design model and the results of the implementation ( $P_{u,DM}$ ) are compared to the experimental results ( $P_{u,EXP}$ ) collected in literature. Likewise, the load-bearing capacity of the same walls are computed using the provisions of EN 1996-1-1 for thin mortared masonry structures ( $P_{u,EC6}$ ). The shape factor and the coefficient K related to the block material have been defined following the provisions of EN 1996-1-1. The brief summary of the parameters used for the implementation of the design model, the results of the experimental tests collected in literature and the load-bearing capacity computed with both approaches are all gathered in Table 4. Upon the computation of the load-bearing capacity of the masonry walls, the safety factor of the concrete material  $\gamma_M$  was set equal to 1,0, since the results of the prediction were intended to be compared to the experimental results.

At the analysis of the results, it is found that the proposed design model is conservative. Indeed, a ratio between the prediction  $P_{u,DM}$  and the experimental results  $P_{u,EXP}$  respectively for each wall gives a mean value of 93%, which means that the proposed design model estimates the actual load-bearing capacity of dry-stacked masonry walls with a satisfactory accuracy. This is of course due to the capacity of the design model to include the negative impact of the geometric imperfections on the overall wall resistance. Indeed, it has been demonstrated that the block imperfections act against the development of the load-bearing capacity of dry-stacked masonry wall by strongly reducing the contact behaviour in walls.

In the same time, the provisions of EN 1996-1-1 for thin-mortared masonry structures overestimate the load-bearing capacity of dry-stacked masonry walls. When the predictions  $P_{u,EC6}$  of EN 1996-1-1 are compared to the experimental results  $P_{u,EXP}$  respectively for each wall, a mean ratio of 131% is found, which means that the load-bearing capacity is overestimated by roughly 31%. This trend could have been expected, as the impacts of block imperfections on the load-bearing capacity of dry-stacked masonry walls are not considered in the current standards. Indeed, the provisions of EN 1996-1-1 are set up for mortared masonry where block imperfections are directly levelled by a mortar layer.

**Table 4: Load-bearing capacity of the wallets and calculation parameters**

Authors in the literature	$\delta_r$	$\delta_h$	Shape factor	K	Height (mm)	Thickness (mm)	Block strength (N/mm <sup>2</sup> )	$P_{u,EXP}$ Experimental (N/mm <sup>2</sup> )	$P_{u,EC6}$ EN 1996-1-1 (N/mm <sup>2</sup> )	$P_{u,DM}$ Design model (N/mm <sup>2</sup> )	Accuracy of the design model in %
Silva et al. (2015)	0,23	0,52	0,9	0,75	500	140	8,8	3,30	3,68	2,95	<b>89%</b>
Silva et al. (2015)	0,23	0,52	0,9	0,75	500	140	12	4,60	4,61	3,95	<b>86%</b>
Sturm et al. (2015)	0,23	0,30	0,9	0,75	810	140	1,96	0,53	1,02	0,50	<b>94%</b>
Drysdale et al. (1991)	0,23	0,52	1,15	0,65	812	203	10,30	3,90	4,72	3,93	<b>101%</b>
Jaafar et al. (2006)	0,23	0,37	1,25	0,65	1200	150	15,20	5,90	6,56	4,56	<b>77%</b>
Thanoon et al (2007, 2014)	0,23	0,27	1,25	0,65	3000	150	17,20	3,89	5,67	3,02	<b>78%</b>
Agaajani et al. (2015)	0,23	0,37	1,25	0,65	1250	200	26,30	5,35	8,40	5,64	<b>105%</b>

## 5 Conclusion

The present research focusses on the assessment of a mitigation strategy to overcome the impact of the geometric imperfections of blocks on the load-bearing capacity of dry-stacked masonry walls and the development of a design model proper to such walls. Experimental tests were performed on masonry wallets and prisms to evidence the efficiency of an additional layer made of well-defined properties to improve the load-bearing capacity of dry-stacked masonry walls. Furthermore, the experimental results were combined with a deterministic statistical model for developing a design model. The efficiency of the design model was discussed in terms of accuracy in the prediction of the load-bearing capacity with respect to the actual value obtained following experiments. In a nutshell, it was found that:

- For engineering purpose, the most relevant improvement of the load-bearing capacity of dry-stacked masonry walls was obtained with the blocks having an additional layer made with a mixture which has a Young's Modulus of 7000 MPa and a mean compressive strength of 38 MPa. They provided up to 31,9% of additional load carrying capacity.
- The design model exhibited an accuracy varying between 77 and 105%, with a mean of 93% in the prediction of the load-bearing capacity of dry-stacked masonry walls.

[Acknowledgements] The authors wholeheartedly thank "Contern - Lëtzebuerger Beton" for the financial support throughout this project. The authors also acknowledge the laboratory technicians of the University of Luxembourg for their commitment during the designing and execution of the experimental tests.

## [References]

- Abang Ali, A. K. (1987). Strength properties and structural performance of interlocking hollow block walls. *J. Inst. Jurutera Malya*, 53, 25–35.
- Agaajani, S., Waldmann, D., Scholzen, F., & Louge, A. (2016). Numerical analysis for the determination of stress percolation in dry-stacked wall systems. *Masonry International*, 29(2), 27–38.

- Allaoui, S., Rekik, A., Gasser, A., Blond, E., & Andreev, K. (2018). Digital Image Correlation measurements of mortarless joint closure in refractory masonry. *Construction and Building Materials*, 162, 334–344. <https://doi.org/10.1016/j.conbuildmat.2017.12.055>
- Anand, K. B., & Ramamurthy, K. (2003). Laboratory-Based Productivity Study on Alternative Masonry Systems. *Journal of Construction Engineering and Management*, 129(3), 237–242. [https://doi.org/10.1061/\(asce\)0733-9364\(2003\)129:3\(237\)](https://doi.org/10.1061/(asce)0733-9364(2003)129:3(237))
- Andreev, K., Sinnema, S., Rekik, A., Allaoui, S., Blond, E., & Gasser, A. (2012). Compressive behaviour of dry joints in refractory ceramic masonry. *Construction and Building Materials*, 34, 402–408. <https://doi.org/10.1016/j.conbuildmat.2012.02.024>
- Bari, N. A. A., Abdullah, N. A., Yusuff, R., Ismail, N., & Jaapar, A. (2012). Environmental Awareness and Benefits of Industrialized Building Systems (IBS). *Procedia - Social and Behavioral Sciences*, 50(July), 392–404. <https://doi.org/10.1016/j.sbspro.2012.08.044>
- Ben Ayed, H., Limam, O., Aidi, M., & Jelidi, A. (2016). Experimental and numerical study of Interlocking Stabilized Earth Blocks mechanical behavior. *Journal of Building Engineering*, 7, 207–216. <https://doi.org/10.1016/j.jobe.2016.06.012>
- Bigoni, D., & Noselli, G. (2010a). Localized stress percolation through dry masonry walls. Part I - Experiments. *European Journal of Mechanics, A/Solids*, 29(3), 291–298. <https://doi.org/10.1016/j.euromechsol.2009.10.009>
- Bigoni, D., & Noselli, G. (2010b). Localized stress percolation through dry masonry walls. Part II - Modelling. *European Journal of Mechanics, A/Solids*, 29(3), 299–307. <https://doi.org/10.1016/j.euromechsol.2009.10.013>
- BS EN 772-1:2000, Methods of test for masonry units – Part 1: Determination of compressive strength.*
- Cetholic. (1988). Mortarless Masonry - The Mecano System. *Housing Science*, 12(2), 145–157.
- Chewe Ngapeya, Gelen Gael, & Waldmann, D. (2020). Overcome of bed-joint imperfections and improvement of actual contact in dry-stacked masonry. *Construction and Building Materials*, 233, 117173. <https://doi.org/10.1016/j.conbuildmat.2019.117173>
- Chewe Ngapeya, Gelen Gaël, & Waldmann, D. (2020). Experimental and analytical analysis of the load-bearing capacity  $P_u$  of improved dry-stacked masonry. *Journal of Building Engineering*, 27(May 2019). <https://doi.org/10.1016/j.jobe.2019.100927>
- Chewe Ngapeya, Gelen Gael, Waldmann, D., & Scholzen, F. (2018). Impact of the height imperfections of masonry blocks on the load bearing capacity of dry-stack masonry walls. *Construction and Building Materials*, 165, 898–913. <https://doi.org/10.1016/j.conbuildmat.2017.12.183>
- Gasser, A., Terny-Rebeyrotte, K., & Boisse, P. (2004). Modelling of joint effects on refractory lining behaviour. *Proceedings of the Institution of Mechanical Engineers, Part L: Journal of Materials: Design and Applications*, 218(1), 19–28. <https://doi.org/10.1243/146442004322849881>
- Haener. (1984). Stacking Mortarless Block System. *Engineering Design Manual*.
- Jaafar, M. S., Thanoon, W. A., Najm, A. M. S., Abdulkadir, M. R., & Ali, A. A. A. (2006). Strength correlation between individual block, prism and basic wall panel for load bearing interlocking mortarless hollow block masonry. *Construction and Building Materials*, 20(7), 492–498. <https://doi.org/10.1016/j.conbuildmat.2005.01.046>
- Kang-Ho Oh; Harry G. Harries; Ahmed A. Hamid. (1995). Behavior of Interlocking Mortarless Masonry Under

Compressive Loads. *Seventh Canadian Masonry Symposium*, 340–352.

Lourenço, P. B., Oliveira, D. V., Roca, P., & Orduña, A. (2005). Dry Joint Stone Masonry Walls Subjected to In-Plane Combined Loading. *Journal of Structural Engineering*, 131(11), 1665–1673. [https://doi.org/10.1061/\(asce\)0733-9445\(2005\)131:11\(1665\)](https://doi.org/10.1061/(asce)0733-9445(2005)131:11(1665))

Lourenço, P. B., & Ramos, L. F. (2004). Characterization of Cyclic Behavior of Dry Masonry Joints. *Journal of Structural Engineering*, 130(5), 779–786. [https://doi.org/10.1061/\(asce\)0733-9445\(2004\)130:5\(779\)](https://doi.org/10.1061/(asce)0733-9445(2004)130:5(779))

Mohamad, G., Fonseca, F. S., Vermeltfoort, A. T., Martens, D. R. W., & Lourenço, P. B. (2017). Strength, behavior, and failure mode of hollow concrete masonry constructed with mortars of different strengths. *Construction and Building Materials*, 134, 489–496. <https://doi.org/10.1016/j.conbuildmat.2016.12.112>

Mohd Saleh Jaafar; Ahmed Alwathaf; Waleed Thanoon; J. Noorzaei; M. R. Abdulkadir. (2006). Behaviour of interlocking mortarless block masonry. *Construction Materials*, 159, 111–117.

Silva, R. A., Soares, E., Oliveira, D. V., Miranda, T., Cristelo, N. M., & Leitão, D. (2015). Mechanical characterisation of dry-stack masonry made of CEBs stabilised with alkaline activation. *Construction and Building Materials*, 75, 349–358. <https://doi.org/10.1016/j.conbuildmat.2014.11.038>

Sturm, T., Ramos, L. F., & Lourenço, P. B. (2015). Characterization of dry-stack interlocking compressed earth blocks. *Materials and Structures/Materiaux et Constructions*, 48(9), 3059–3074. <https://doi.org/10.1617/s11527-014-0379-3>

Tang, F. (2012). Effect of mortar joint thickness on the compressive strength of autoclaved flyash-lime brick masonry. *Applied Mechanics and Materials*, 190–191, 462–466.

Thallon R. (1983). Dry-Stack Block. *Fine Homebuilding Magazine*, 50–57.

Thanoon, W. A., Jaafar, M. S., Abdul Kadir, M. R., Abang Ali, A. A., Trikha, D. N., & Najm, A. M. S. (2004). Development of an innovative interlocking load bearing hollow block system in Malaysia. *Construction and Building Materials*, 18(6), 445–454. <https://doi.org/10.1016/j.conbuildmat.2004.03.013>

Thanoon, W. A. M., Alwathaf, A. H., Noorzaei, J., Jaafar, M. S., & Abdulkadir, M. R. (2008). Finite element analysis of interlocking mortarless hollow block masonry prism. *Computers and Structures*, 86(6), 520–528. <https://doi.org/10.1016/j.compstruc.2007.05.022>

Vasconcelos, G., & Lourenço, P. B. (2009). Experimental characterization of stone masonry in shear and compression. *Construction and Building Materials*, 23(11), 3337–3345. <https://doi.org/10.1016/j.conbuildmat.2009.06.045>

Zahra, T., & Dhanasekar, M. (2018). Characterisation and strategies for mitigation of the contact surface unevenness in dry-stack masonry. *Construction and Building Materials*, 169, 612–628. <https://doi.org/10.1016/j.conbuildmat.2018.03.002>

Zucchini, A., & Lourenço, P. B. (2007). Mechanics of masonry in compression: Results from a homogenisation approach. *Computers and Structures*, 85(3–4), 193–204. <https://doi.org/10.1016/j.compstruc.2006.08.054>